J|A|C|S
ARTICLES
Published on Web 09/27/2006

Early Events in the Photochemistry of Aryl Azides from Femtosecond UV/Vis Spectroscopy and Quantum Chemical Calculations

Gotard Burdzinski,[†,‡] John C Hackett,[‡] Jin Wang,[‡] Terry L. Gustafson,[‡] Christopher M. Hadad,*[,‡] and Matthew S. Platz*[,‡]

Contribution from the Quantum Electronics Laboratory, Faculty of Physics, Adam Mickiewicz University, 85 Umultowska, Poznan 61-614, Poland, and Department of Chemistry, The Ohio State University, 100 West 18th Avenue, Columbus, Ohio 43210

Received March 5, 2006; E-mail: hadad.1@osu.edu; platz.1@osu.edu

Abstract: The photochemistry of *para*- and *ortho*-biphenylyl azides and 1-naphthyl azide was studied by ultrafast spectroscopy. In every case, the singlet azide second excited states were observed by transient absorption spectroscopy and were found to have lifetimes of hundreds of femtoseconds. The decay of the S_2 states of the azides was accompanied by the growth of transient absorption of the corresponding singlet nitrenes. The intermediate S_1 state of the azides could not be observed due to its low instantaneous concentration resulting from fast fragmentation and nitrene formation. Quantum chemical calculations predict that the S_2 state of the azide is bound and that there is a much lower barrier toward arylnitrene formation from the S_1 state of the azide. Vibrational cooling of *para*-biphenylnitrene (11 ps) was experimentally observed. The lifetime of singlet *ortho*-biphenylnitrene was 16 ps in acetonitrile and was not affected by perdeuteration of the aryl ring. The lifetime of singlet 1-naphthylnitrene is 12 ps in acetonitrile at ambient temperature.

I. Introduction

Photolysis of aryl azides promotes nitrogen extrusion and the release of singlet nitrenes.[1] The chemistry of arylnitrenes has been extensively studied by chemical, physical, and computational methods.[2] The quantum yields of light-induced decomposition of the naphthyl azides are close to unity, and that of simple phenyl azides falls in the range of 0.1−0.7 and depends on the concentration of the azide.[3] To our knowledge, simple phenyl, biphenylyl, and naphthyl azides are not known to have any observable fluorescence, which is consistent with their large quantum yields for extrusion of molecular nitrogen. Otherwise, essentially nothing is known of the details by which aryl azide excited states decompose to form singlet nitrenes. The development of ultrafast spectroscopic techniques[4] and modern quantum chemical computational methods provides tools with which to begin to understand how the excited-state surface of the aryl azides connects to the ground-state surfaces of the nitrenes. In this paper, we describe the application of ultrafast transient absorption spectroscopy to the study of the photochemistry of *para*- and *ortho*-biphenylyl azides (**PBA** and **OBA**, respectively) and 1-naphthyl azide (**1NA**) and report the observation of the S_2 azide excited states and lifetimes and the spectra and lifetimes of the corresponding singlet aryl nitrenes in acetonitrile solution at ambient temperature.

II. Results and Discussion

II.1. Computational Chemistry: Ground-State Equilibrium Geometries and Vertical Excitation Energies and Electron Densities. The singlet ground (S_0) states of **1NA** (Figure 1), **PBA**, **OBA** (Figure 2), and phenyl azide (**PA**, Supporting Information) were optimized at the RI-CC2[5] and B3LYP[6] levels of theory. **1NA** and **PA** were optimized with C_s symmetry. Optimizations performed without symmetry restraints remained C_s symmetric, and therefore only the results obtained with C_s species will be described here. Vertical excitation energies, oscillator strengths, and the primary occupied and virtual orbitals contributing to the lowest energy singlet excitations are listed in Table 1.

[†] Adam Mickiewicz University.
[‡] The Ohio State University.

(1) (a) Lwowski, W., Ed. *Nitrenes*; Wiley: New York, 1970. (b) Scriven, E. F. V. *Azides and Nitrenes*; Academic Press: New York, 1984.
(2) (a) Gritsan, N. P.; Platz, M. S. *Adv. Phys. Org. Chem.* **2001**, *36*, 255. (b) Platz, M. S. Nitrenes. In *Reactive Intermediates Chemistry*; Moss, R. A., Platz, M. S., Jones, M., Jr., Eds.; Wiley: New York, 2004; pp 501−560. (c) Schuster, G. B.; Platz, M. S. *Adv. Photochem.* **1992**, *17*, 69−143.
(3) (a) Budyka, M. F.; Biktimirova, N. V.; Gavrishova, T. N.; Laukhina, O. D. *Russ. J. Phys. Chem.* **2005**, *79*, 1666. (b) Avramenko, L. F.; Eshchenko, N. P.; Kondratenko, P. A.; Novikova, E. A.; Syromyatnikov, V. G. *Ukr. Khim. Zh. (Russ. Ed.)* **2005**, *71*, 64. (c) Budyka, M. F.; Kantor, M. M.; Alfimov, M. V. *Izv. Akad. Nauk, Ser. Khim.* **1992**, *3*, 752. (d) Jenkins, R. F.; Waddell, W. H.; Richter, H. W. *J. Am. Chem. Soc.* **1987**, *109*, 1583. (e) Geiger, M. W.; Elliot, M. M.; Karacostas, V. D.; Moricone, T. J.; Salmon, J. B.; Sideli, V. L.; St. Onge, M. A. *Photochem. Photobiol.* **1984**, *40*, 545. (f) Koryttsev, K. Z.; Oleinik, A. V.; Zhurnal, M. *Fiz. Khim.* **1973**, *47*, 700. (g) Koryttsev, K. Z.; Oleinik, A. V.; Korshuniv, I. A. *Tr. Khim. Khim. Tekhnol.* **1971**, *1*, 207.
(4) Rulliere, C. *Femtosecond Laser Pulses*; Springer-Verlag: Berlin, Heidelberg, 1998.
(5) (a) Hättig, C.; Weigend, F. *J. Chem. Phys.* **2000**, *113*, 5154. (b) Hättig, C.; Weigend, F. *J. Chem. Phys.* **2000**, *113*, 5154.
(6) (a) Becke, A. D. *Phys. Rev. A* **1988**, *38*, 3098. (b) Becke, A. D. *J. Chem. Phys.* **1993**, *98*, 5648. The version of the B3LYP density functional used includes VWN-V rather than VWN-III. (c) Lee, C.; Yang, W.; Parr, R. G. *Phys. Rev. B* **1988**, *37*, 785.

10.1021/ja061520i CCC: $33.50

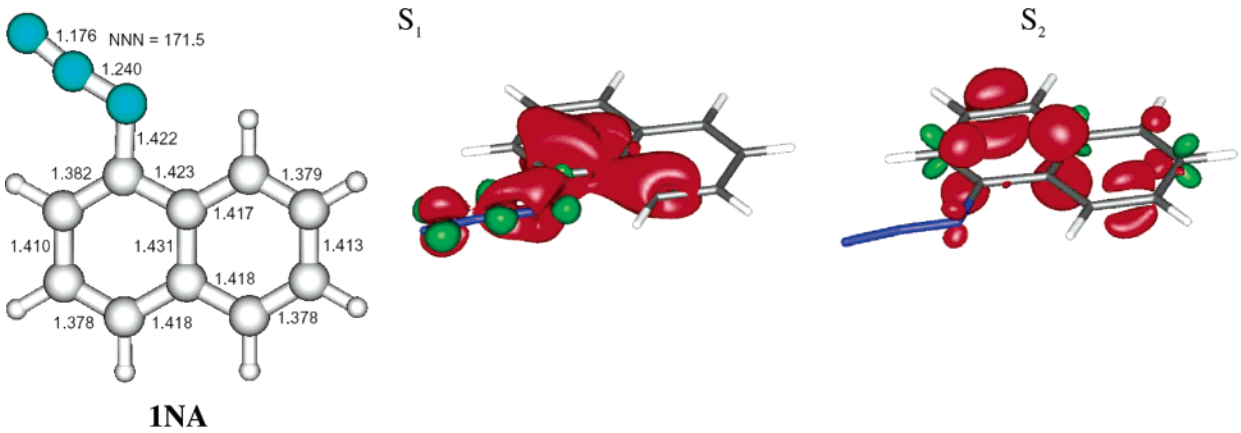

Figure 1. RI-CC2/TZVP 1-naphthyl azide S_0 optimized geometry and excited-state difference density plots (S_1 and S_2 densities less the ground-state density). A red surface surrounds areas where electron density is depleted from S_0; a green surface surrounds areas where electron density is accumulated in the excited state. Bond distances and angles are listed in angstroms and degrees, respectively. S_1 and S_2 plots are plotted with isocontour values of ± 0.02 and ± 0.005 a.u., respectively.

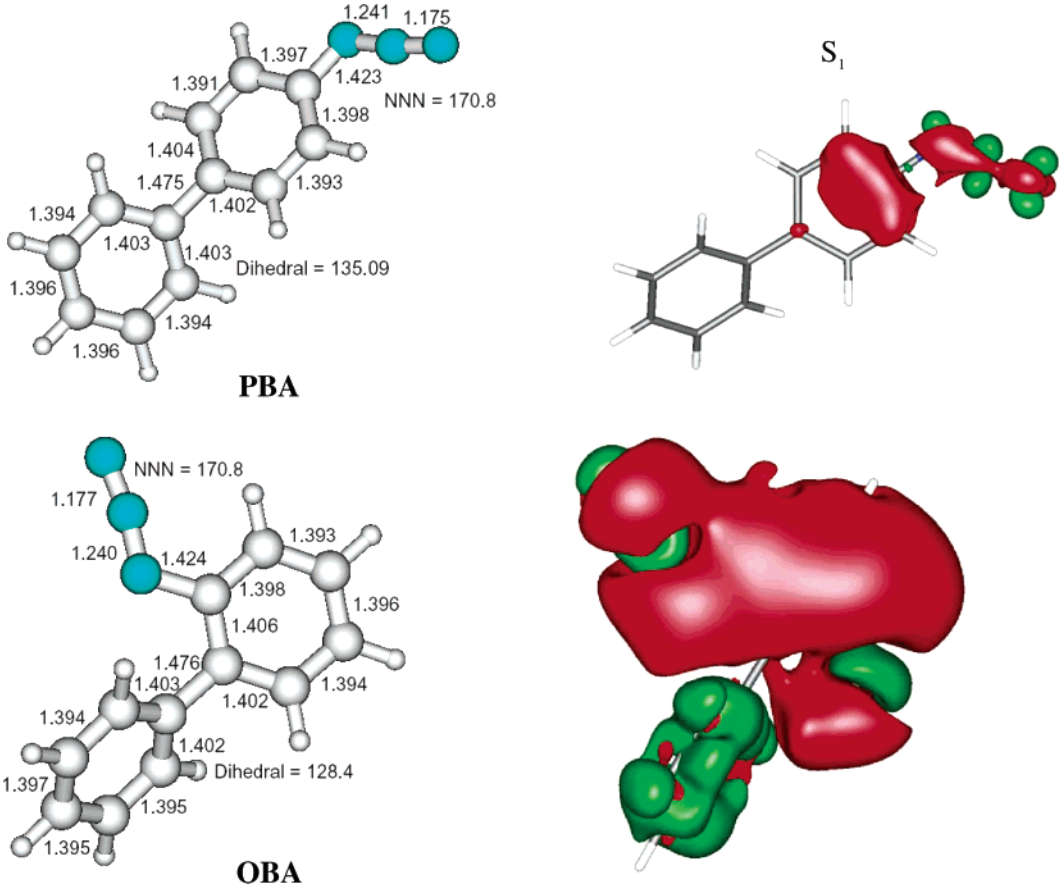

Figure 2. RI-CC2/TZVP biphenylyl azide S_0 optimized geometries and S_1 excited-state difference density plots (S_1 densities less the ground-state densities). A red surface surrounds areas where electron density is depleted from S_0; a green surface surrounds areas where electron density is accumulated in the excited state. Bond distances and angles are listed in angstroms and degrees, respectively. Surfaces are plotted with isocontour values of ± 0.02 a.u.

Contour surfaces for these orbitals are presented in the Supporting Information (as well as a more complete list of higher energy excitations). Transitions corresponding to the second excited states (S_2) are characterized by oscillator strengths, which are one or two orders of magnitude greater than those for the first excited state (S_1). Inspection of the orbitals involved in the excitations reveals that the second excited state (S_2) is characterized by a $\pi \rightarrow (\pi^*,\text{aryl})$ transition in which the π^* orbital is localized on the aryl ring, whereas the first excited state (S_1) is characterized by a $\pi \rightarrow$ (in-plane,π^*,azide) orbital transition in which the π^* orbital is localized on the azide unit. However, because these transitions have multiconfigurational character, electron redistribution as a result of excitation requires consideration of the total electron densities for the ground and excited states.

One can visualize such electron redistribution by the use of a difference density between the excited and the ground state (using the S_0 geometry). The difference densities at the RI-CC2 level for the first (S_1) and second (S_2) excited states relative to the ground state are depicted in Figures 1 and 2 for 1-naphthyl

Table 1. RI-CC2 and TD-B3LYP Aryl Azide Vertical Excitation Energies[a]

	TD-B3LYP			RI-CC2		
state	character	energy/eV (nm)	oscillator strength	character	energy/eV (nm)	oscillator strength
			Phenyl Azide (**PA**)			
1	5a″ → 27a′	3.92 (316)	1.68×10^{-5}	5a″ → 27a′	4.36 (284)	5.33×10^{-4}
2	5a″ → 6a″	4.82 (257)	8.21×10^{-2}	5a″ → 7a″	4.96 (250)	2.13×10^{-2}
			1-Naphthyl Azide (**1NA**)			
1	7a″ → 38a′	3.70 (335)	1.98×10^{-4}	7a″ → 38a′	4.28 (290)	4.74×10^{-4}
2	7a″ → 8a″	3.97 (312)	1.75×10^{-1}	7a″ → 9a″	4.34 (286)	2.24×10^{-2}
			p-Biphenylyl Azide (**PBA**)			
1	51a → 53a	3.78 (328)	2.06×10^{-4}	51a → 53a	4.29 (289)	1.02×10^{-3}
2	51a → 52a	4.37 (284)	6.63×10^{-1}	51a → 54a	4.74 (262)	7.20×10^{-2}
			o-Biphenylyl Azide (**OBA**)			
1	51a → 53a	3.88 (320)	7.47×10^{-4}	51a → 54a	4.36 (284)	5.09×10^{-4}
2	51a → 54a	4.50 (276)	3.03×10^{-2}	51a → 53a	4.74 (262)	2.20×10^{-2}

[a] Using the corresponding fully optimized ground-state (S_0) geometry at the same level of theory for determining the excited states.

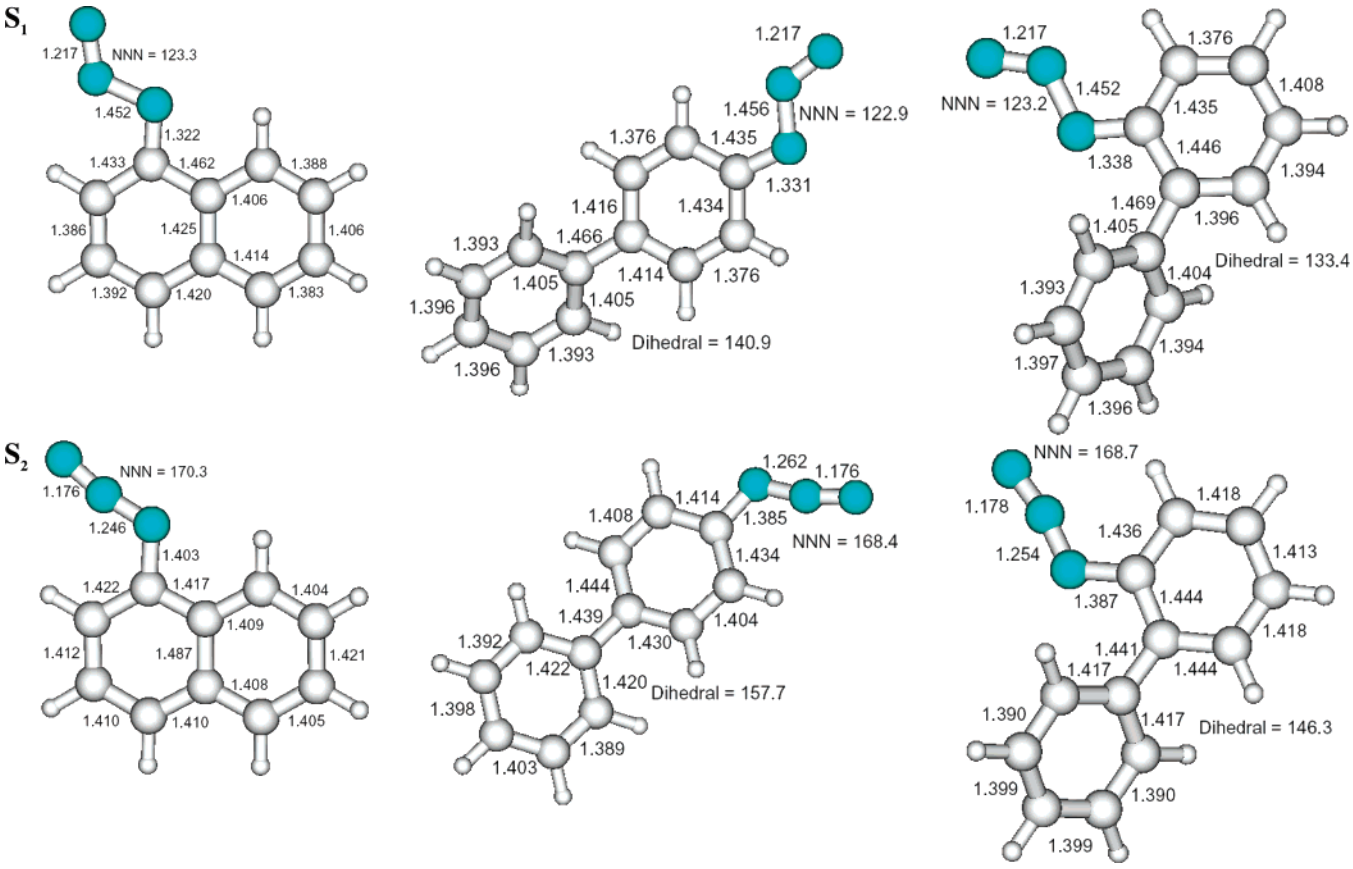

Figure 3. RI-CC2/TZVP aryl azide excited-state equilibrium geometries. Bond distances and angles are listed in angstroms and degrees, respectively.

azide and the biphenylyl azides, respectively. In those figures, green contours correspond to electron density accumulation in the excited state, and red contours correspond to depletion from S_0. Difference densities of the second excited states reveal a redistribution of electron density, which is localized to the aryl's π system and for which there is no appreciable change in electron density for the azide moiety. In contrast, electron redistribution in the first excited state is characterized by a depletion of electron density from the aryl azide's π system and in the region of the N−N bond proximal to the naphthalene unit. Loss of electron density in the proximal N−N bonding region is consistent with expulsion of N_2 in the first excited state, as will be discussed later. (TD-B3LYP[7] difference densities are presented in the Supporting Information.)

II.2. Excited-State Equilibrium Geometries and Potential Energy Surfaces. Using the recent implementation of RI-CC2 analytical gradients for excited states, the equilibrium geometries for the first and second excited states of each aryl azide were computed. Attempts to optimize the excited states' geometries using time-dependent density functional theory at the TD-B3LYP level failed due to instabilities in the DFT reference wave function as the proximal N−N bond lengthened in the first excited state. Therefore, the discussion here will be limited to the RI-CC2 results. Equilibrium geometries of the first and second excited states are displayed in Figure 3. With the exception of modest changes in bond lengths, the geometries

(7) (a) Furche, F.; Ahlrichs, R. *J. Chem. Phys.* **2002**, *117*, 7433. (b) Furche, F.; Ahlrichs, R. *J. Chem. Phys.* **2004**, *121*, 12772.

of the aryl azides' second excited state (S_2) are similar to those of the ground state. However, there is an increased coplanarity of the phenyl rings in the S_1 and S_2 states of the biphenylyl azides. In contrast, the first excited state (S_1) is characterized by a remarkable lengthening of the proximal N−N bond and bending of the azide functionality. All of the aryl azides have a proximal N−N bond length of ∼1.45 Å in the S_1 states, ∼0.2 Å longer than for the S_0 ground state. Two minima on the S_1 surface of phenyl azide (**PA**) were identified. The first has a cisoid arrangement of atoms about the proximal N−N bond, while the second geometry is transoid. The proximal N−N bond in the cisoid species is somewhat longer with a distance of 1.51 Å. However, the RI-CC2 calculations demonstrate that the transoid azide is energetically preferred by 9.5 kcal/mol relative to the cisoid S_1 for **PA**. We optimized both cisoid and transoid S_0/S_1 conical intersections (CI) for phenyl azide at the CASSCF(4,6)/SVP level of theory (Supporting Information). At this theoretical level, the transoid CI is favored energetically by 10.2 kcal/mol. Both conical intersections share geometric features similar to those of the S_1 intermediate that was optimized at the RI-CC2/TZVP level of theory. Of particular interest is the proximal N−N bond length. The cisoid and transoid conical intersections have N−N bond lengths of 1.47 and 1.44 Å, respectively. These data suggest that a nearby S_0/S_1 conical intersection in **PA** (and, by analogy, related aryl azides) could provide an avenue for the decay of the S_1 state back to the S_0 surface. For this reason, we do not expect the cisoid species to be the major contributor to the observed chemistry on the S_1 surface. The lengthening of the proximal N−N bond is consistent with the depletion of electron density in this region as observed in the excited states' difference density plots (see Figures 1 and 2).

Furthermore, given the electron redistribution that occurred in the first excited state as well as the lengthening of the proximal N−N bond, we hypothesized that the first excited state may be dissociative to form molecular nitrogen and the corresponding singlet arylnitrene. To compute approximate barriers for N_2 expulsion on the ground and excited states' potential energy surfaces, the proximal N−N bonds for the respective equilibrium geometries were stretched incrementally and the energy was computed to generate potential energy profiles for the various surfaces. Because the remaining internal coordinates of the aryl azides were not relaxed as the proximal N−N bond was stretched, the resulting approximate energy barriers represent the upper bound for this process.

Nonrelaxed (rigid) potential energy curves for N_2 expulsion from the aryl azides are shown in Figure 4. Energetic barriers for N_2 expulsion on the S_0 ground-state surface are consistently >60 kcal/mol for the three aryl azides. Experimental activation energies to the decomposition of aryl azides are much smaller as, for example, the activation energies to decomposition of 1- and 2-naphthyl azides are 34.1 and 38.1 kcal/mol, respectively.[8] For comparison, fully relaxed computational studies show *para*-biphenylyl azide's decomposition to singlet *para*-biphenylnitrene and molecular nitrogen is 40.2 kcal/mol at the RI-CC2 level of theory. This difference indicates that the rigid scan noted above is, as expected, an upper limit to the dissociation barrier. In the second excited states (S_2), N_2 expulsion in the naphthyl azides

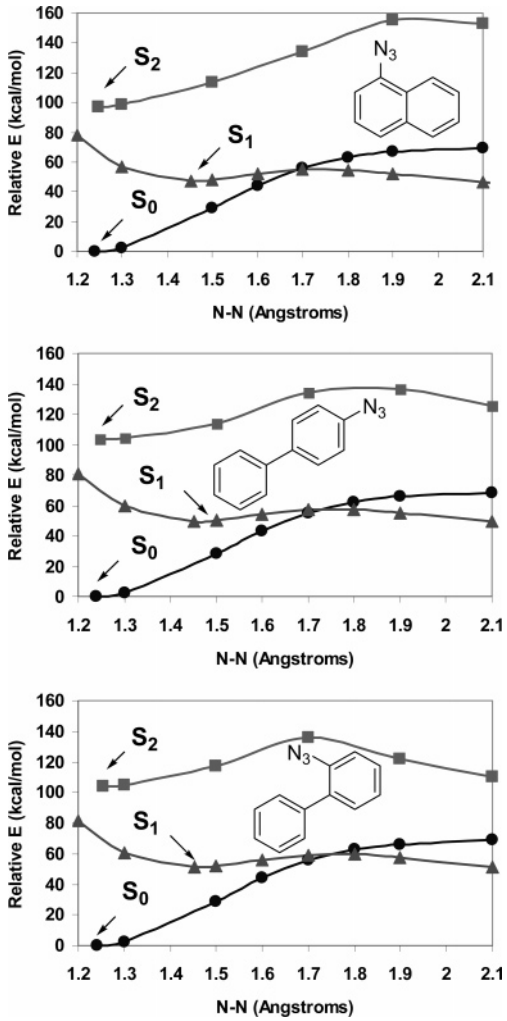

Figure 4. Aryl azide RI-CC2/TZVP rigid potential energy curves for N_2 expulsion. Ground state (●), first excited state (▲), and second excited state (■). The arrows indicate the N−N bond length of the fully optimized stationary point on each respective energy surface.

was comparable to the ground state, yielding barriers of ∼58−59 kcal/mol (and, once again, reflects an upper limit to the dissociation energy due to the rigid scan). The biphenylyl azides, however, demonstrated somewhat lower barriers of ∼32−33 kcal/mol for the S_2 surfaces. Consistent with our hypothesis stated above, however, is that the first excited state (S_1) of all three azides examined is dissociative toward the formation of the singlet arylnitrene and N_2, and the computed (upper limit) barrier is 7−9 kcal/mol for dissociation on the S_1 surface. A S_0/S_1 state crossing occurs in the excited-state potential surface manifolds for these aryl azides when the N−N coordinate is ∼1.7 Å. This state crossing provides an avenue for the S_1 state to return to S_0 without dissociation. This may account for the slightly less than unit quantum yields of decomposition of simple phenyl azides.[3]

As previously discussed, rigid scans provide an upper limit to the dissociation barrier to form the singlet arylnitrene and N_2. To verify the properties of the potential energy surface derived from the rigid scan, we performed a fully relaxed potential energy surface scan of the N−N coordinate in **1NA** (Figure 5). In general, the features of the ground and excited states' potential energy surfaces are similar to those obtained from the rigid scan, but there are some important differences.

(8) (a) Boshev, G.; Dyall, L. K. *Aust. J. Chem.* **1972**, *25*, 599. (b) Boshev, G.; Dyall, L. K. *J. Chem. Soc. B* **1968**, 976.

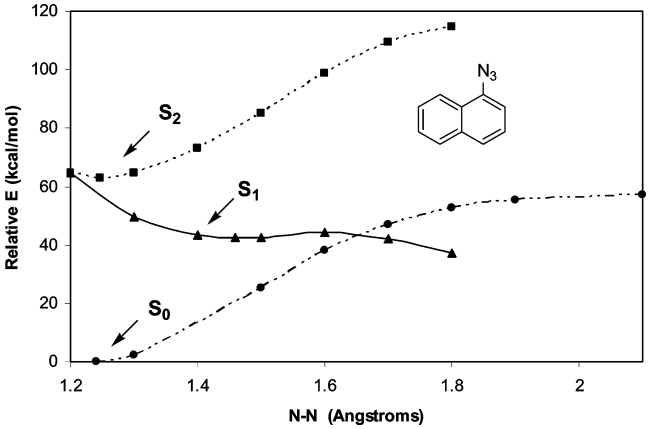

Figure 5. RI-CC2/TZVP fully relaxed potential energy curves for N_2 expulsion in 1-naphthyl azide. Ground state (●), first excited state (▲), and second excited state (■). The arrows indicate the N−N bond length of the fully optimized stationary point on each respective energy surface.

The barrier for expulsion of N_2 on the S_0 surface is ∼55 kcal/mol. On the S_2 surface, the barrier for N_2 expulsion is ∼52 kcal/mol, similar to the value computed for the S_0 surface. One feature that was not immediately apparent was the shallow nature of the S_2 potential energy surface in the vicinity of its equilibrium bond length. The fully relaxed scan of the N−N coordinate on the S_1 surface further supports the hypothesis that this state is dissociative. The barrier for N_2 expulsion is reduced to ∼2 kcal/mol. The S_0/S_1 state crossing occurs at the slightly shorter N−N distance of ∼1.65 Å. A very interesting feature of the fully relaxed S_1 potential energy surface is the presence of an intersection with the S_2 surface near the Frank-Condon point at ∼1.2 Å. Taken together with the shallowness of the potential energy surface in this region, it appears that S_2 can couple vibronically to S_1 near the S_0 geometry, thus providing a route for decay of electronically excited S_2 state to the lower energy S_1 surface.

The calculations (Table 1) predict that the transition of S_0 to S_2 has a much larger oscillator strength than the S_0 to S_1 transition in all of the aromatic azides considered here. Thus, UV excitation of the biphenylyl and naphthyl azides is predicted to promote the ground-state azide to the S_2 state. The S_2 state will deactivate rapidly to the S_1 state of the aromatic azides apparently by vibronic coupling. The S_1 state of the azide will then undergo nitrogen extrusion with a small barrier of ∼2 kcal/mol. This process is highly exothermic (typically by ∼40 kcal/mol), and a vibrationally excited nitrene will be formed. The S_1 state of the azide may also deactivate to the ground state, thereby reducing the efficiency of arylnitrene formation (Scheme 1).

II.3. Ultrafast Spectroscopic Studies of Aromatic Azides. A. *para*-Biphenylyl Azide. The photochemistry of *para*-biphenylyl azide (**PBA**) is summarized in Scheme 2. The initially formed relaxed singlet nitrene **^{1}PBN** has $\lambda_{max} = 343$ nm and τ ∼9 ns at ambient temperature.[9] At ambient temperature, the lifetime of the nitrene is controlled by cyclization to benzazirine **PBAZ**. At 77 K, **^{1}PBN** undergoes intersystem crossing to **^{3}PBN** with rate constant $k_{isc} = (9.3 \pm 0.4) \times 10^6$ s^{-1} in 3-methylpentane.[9] The benzazirines derived from most phenylnitrenes rapidly ring open at ambient temperature to form

Scheme 1

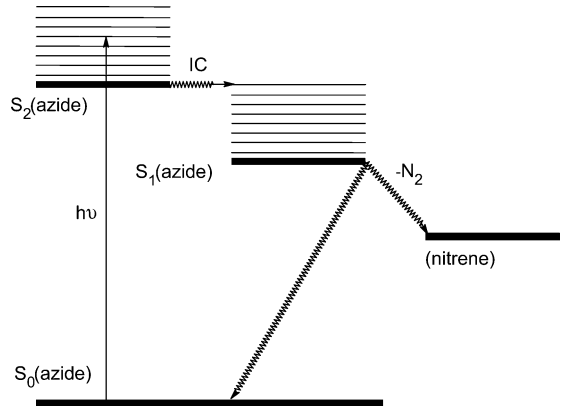

Scheme 2

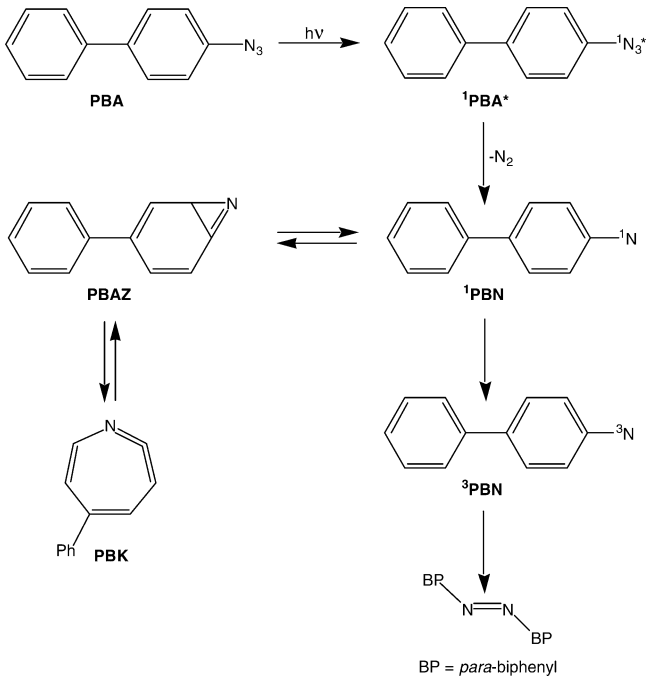

1,2,4,5-azacycloheptatetraenes (also referred to as didehydroazepines or cyclic ketenimines).[2]

Ultrafast LFP of **PBA** ($A = 0.6$ at 266 nm) in acetonitrile at ambient temperature produces the transient spectra shown in Figure 6.[9] There is a broadly absorbing transient at 480 nm that forms within the laser pulse (Figure 6, inset) and decays with a time constant of ∼100 fs. As the transient absorption decays at 480 nm, it grows at 350 nm. The latter species is readily assigned to **^{1}PBN** on the basis of nanosecond time-resolved studies.[10] The precursor of the singlet arylnitrene must be an excited state of the nitrene or azide **^{1}PBA***, which absorbs at 480 nm. This initially detected transient is assigned to the S_2 state of **PBA** on the basis of our calculations for the oscillator strengths and necessary excitation energies, as listed in Table 1.

As expected, relaxed singlet nitrene **^{1}PBN** does not exhibit any significant population decay on the 100 ps time scale (∼9 ns).[6] However, the transient absorption spectrum of the singlet nitrene (**^{1}PBN**) undergoes subtle reshaping within a few

(9) Burdzinski, G.; Gustafson, T. L.; Hackett, J. C.; Hadad, C. M.; Platz, M. S. *J. Am. Chem. Soc.* **2005**, *127*, 13764.

(10) Tsao, M.-L.; Gritsan, N. P.; James, T. R.; Platz, M. S.; Hrovat, D. A.; Borden, W. T. *J. Am. Chem. Soc.* **2003**, *125*, 9343.

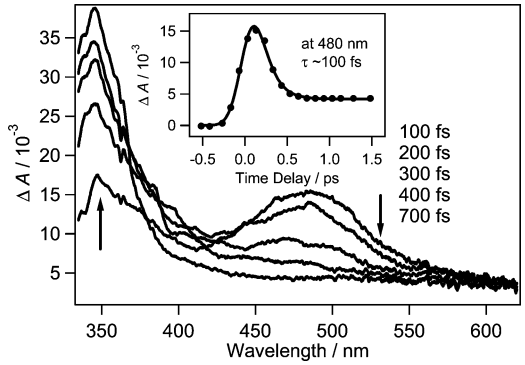

Figure 6. Transient absorption spectra recorded in a 100−700 fs time window for *para*-biphenylyl azide in acetonitrile. The time dependence of the signal at 480 nm is shown in the inset.

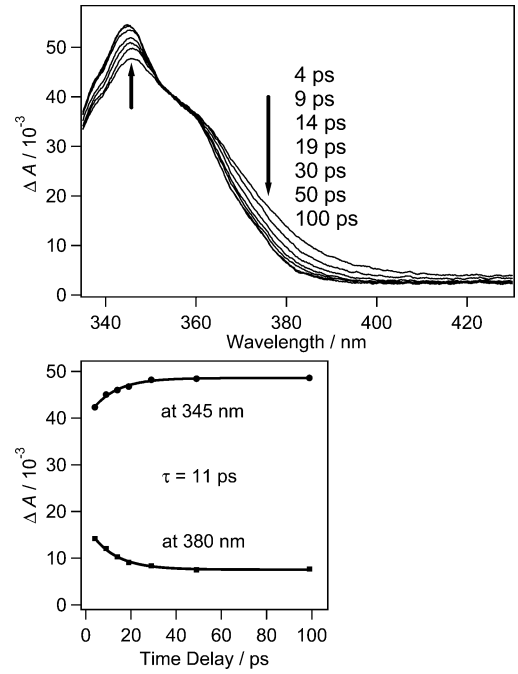

Figure 7. Transient absorption spectra recorded in a 4−100 ps time window for *para*-biphenylyl azide in acetonitrile (upper graph), and selected kinetic traces at 345 nm (●) and 380 nm (■).

picoseconds of the laser pulse as shown in Figure 7. A decay (11 ps) is observed on the red edge (380 nm), and a rise (11 ps) is observed on the blue edge (345 nm) of the absorption band. The time-dependent band narrowing is characteristic of vibrational cooling (VC) of species initially formed with excess vibrational energy.[11] The 11 ps time constant is consistent with other reports of VC of polyatomic molecules. A derivative of **^{1}PBN**, 3,5-dichloro-*ortho*-biphenylnitrene, also undergoes vibrational cooling in cyclohexane with an 11 ps decay time.[12]

B. *ortho*-Biphenylyl Azide. The photochemistry of *ortho*-biphenylyl azide (**OBA**) (Scheme 3) resembles that of the *para*-isomer, but with two distinct differences. First, the *ortho*-phenyl group accelerates cyclization of the singlet nitrene to the corresponding benzazirine.[10] This is still the major route by

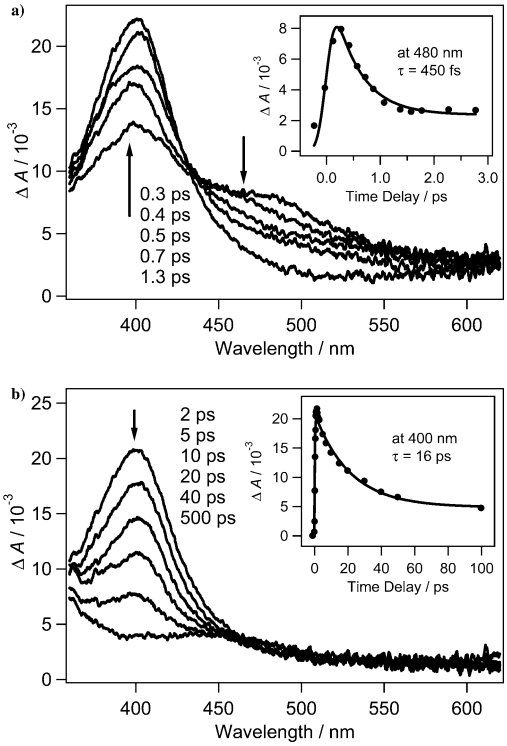

Figure 8. Transient absorption spectra recorded between (a) 0.3−1.3 ps after the laser pulse and with (b) 2−500 ps time windows for *ortho*-biphenylyl azide in acetonitrile. The time dependences of the signal measured at 480 and 400 nm are shown as insets.

which relaxed **^{1}OBN** will decay. Furthermore, relaxed singlet *ortho*-biphenylnitrene (**^{1}OBN**), in addition to forming a benzazarine (**OBAZ**), can also cyclize in a minor process to form isocarbazole (**IC**). Isocarbazole will then undergo a rapid (ns) 1,5-hydrogen migration to form carbazole (**C**).[10] This process is catalyzed by water. Carbazole formation is synthetically useful, and this reaction has stimulated many studies.[13−15] Isocarbazole absorbs strongly in the visible region because of its quinoidal nature, making it an attractive candidate for study by time-resolved methods.[10,12] Singlet **^{1}OBN** has a subnanosecond lifetime at ambient temperature. LFP of **OBA** at 77 K in glassy 3-methylpenatne produces a singlet nitrene with $\lambda_{max} = 410$ nm and $\tau = 59$ ns under cryogenic conditions.[10]

There is a report of an ultrafast study of a related system.[12] Ultrafast LFP of 2-azido-3,5-dichlorobiphenyl produces the expected nitrene ($\lambda_{max} = 425$ nm in cyclohexane); see Scheme 4. Benzazirine formation should be unimportant in this system because the bulky chlorine substituent should retard that reaction. Unsurprisingly, nanosecond and ultrafast LFP produce broad intense absorption of the dichloroisocarbazole with a maximum at 450 nm in cyclohexane. The lifetime of singlet 3,5-dichloro-*ortho*-biphenylnitrene is 260 ps in cyclohexane and is only 62 ps in methanol.

Ultrafast LFP of *ortho*-biphenylyl azide (**OBA**) in acetonitrile ($A = 0.6$ at 266 nm) at ambient temperature produces the

(11) (a) Laermer, F.; Elsaesser, T.; Kaiser, W. *Chem. Phys. Lett.* **1989**, *156*, 38. (b) Miyasaka, H.; Hagihiro, M.; Okada, T.; Mataga, N. *Chem. Phys. Lett.* **1992**, *188*, 259. (c) Schwarzer, D.; Troe, J.; Votsmeier, M.; Zerezke, M. *J. Chem. Phys.* **1996**, *105*, 3121. (d) Elsaesser, T.; Karser, W. *Annu. Rev. Phys. Chem.* **1991**, *42*, 83.
(12) Gritsan, N. P.; Polshakov, D. A.; Tsao, M.-L.; Platz, M. S. *Photochem. Photobiol. Sci.* **2005**, *4*, 23.
(13) (a) Smith, P. A. S.; Brown, B. B. *J. Am. Chem. Soc.* **1951**, *73*, 2438. (b) Smith, P. A. S.; Brown, B. B. *J. Am. Chem. Soc.* **1951**, *73*, 2435. (c) Smith, P. A. S.; Hall, J. H. *J. Am. Chem. Soc.* **1962**, *84*, 1632.
(14) Lehman, P. A.; Berry, R. S. *J. Am. Chem. Soc.* **1973**, *95*, 8614.
(15) (a) Sundberg, R. J.; Brenner, M.; Suter, S. R.; Das, B. P. *Tetrahedron Lett.* **1970**, *31*, 2715. (b) Sundberg, R. J.; Heintzelman, R. W. *J. Org. Chem.* **1974**, *39*, 2546. (c) Sundberg, R. J.; Gillespie, D. W.; DeGraff, B. A. *J. Am. Chem. Soc.* **1975**, *97*, 6193.

Scheme 3

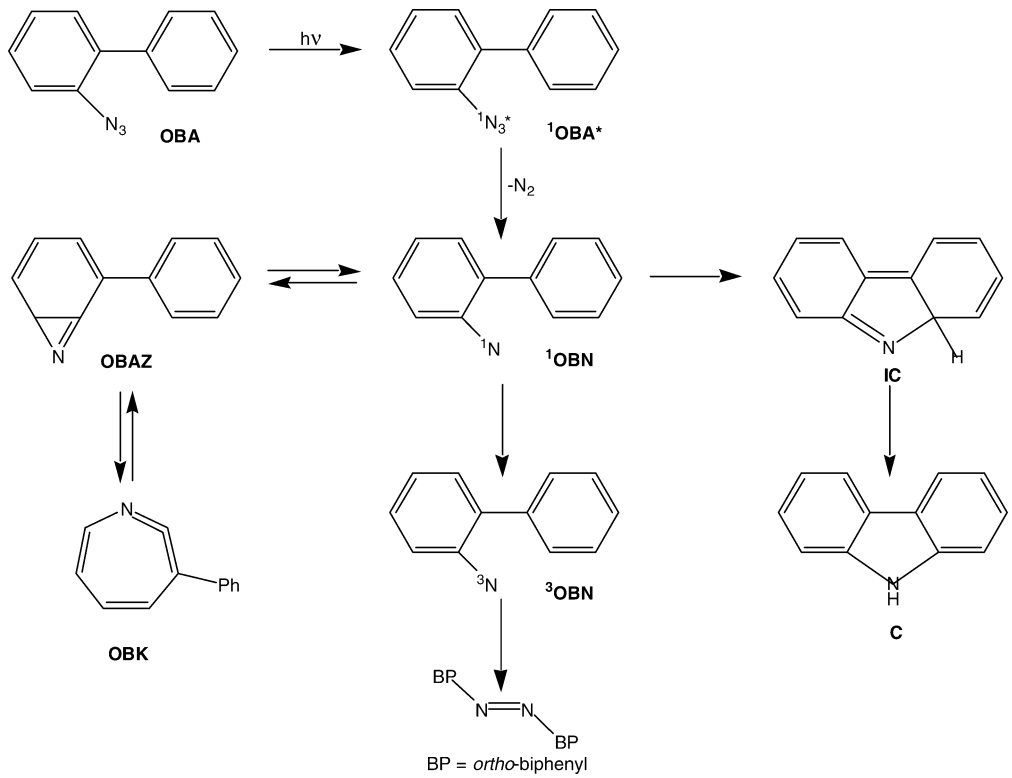

Scheme 4

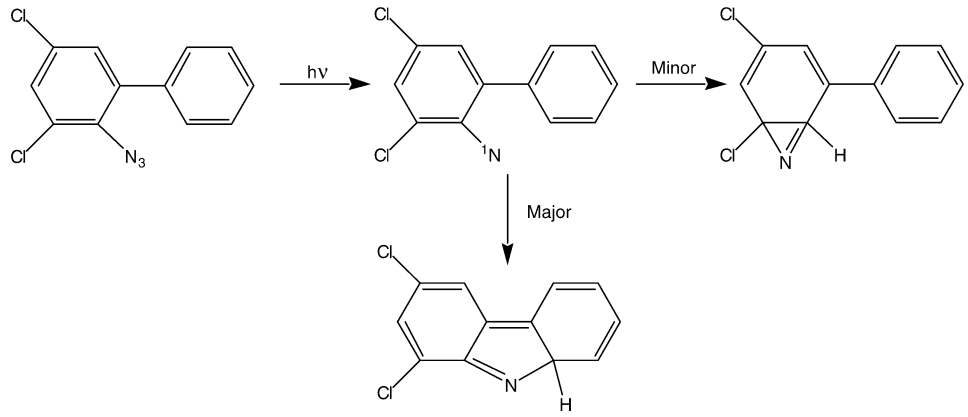

transient spectra in Figure 8.[9] Transient absorption at 480 nm (**^{1}OBA*** in the S_2 state) is formed within the laser pulse and decays with a time constant of 450 ± 150 fs. As this absorption decays, a new absorption at 400 nm (**^{1}OBN**) grows with a time constant of 280 ± 150 fs. There is an isosbestic point at 435 nm. Singlet *ortho*-biphenylnitrene decays with a time constant of 16 ± 3 ps (Figure 8b, inset). The 16 ps time constant represents the population decay of the singlet nitrene (**^{1}OBN**) by isomerization to both isocarbazole and a benzazirine (and subsequently the benzazirine ring expands to form a 1,2-didehydroazepine). The spectrum of **^{1}OBN** does not undergo reshaping characteristic of vibrational cooling, even though the decay of **^{1}OBN** takes place on the time scale of vibrational cooling. Thus, either **^{1}OBN** is formed vibrationally relaxed, or, most likely, we are monitoring the disappearance of **^{1}OBN** before it can shed its excess heat to solvent.

The transient spectrum of isocarbazole, if present at all, is extremely weak, because **^{1}OBN** deactivates mainly to form **OBAZ**.[10] Similar results were obtained upon LFP of *ortho*-biphenylyl azide-d_9. In this case, the lifetime of the perdeuterated **^{1}OBA-d_9** was 450 ± 150 fs, and that of **^{1}OBN-d_9** was 12 ps.

C. 1-Naphthyl Azide. The photochemistry of 1-naphthyl azide has been studied by chemical,[16] physical,[17−19] and computational methods.[19,20] This work provides a coherent mechanistic framework with which to interpret ultrafast experiments.

(16) (a) Hilton, S. E.; Scriven, E. F. V.; Suschitzky, H. *J. Chem. Soc., Chem. Commun.* **1974**, *21*, 853. (b) Carroll, S. E.; Nay, B.; Scriven, E. F. V.; Suschitzky, H. *Synthesis* **1975**, 710. (c) Carroll, S. E.; Nay, B.; Scriven, E. F. V.; Suschitzky, H. *Tetrahedron Lett.* **1977**, 943. (d) Leyva, E.; Platz, M. S. *Tetrahedron Lett.* **1987**, *28*, 11. (e) Carroll, S. E.; Nay, B.; Scriven, E. F. V.; Suschitzky, H.; Thomas, D. R. *Tetrahedron Lett.* **1977**, 3175. (f) Nay, B.; Scriven, E. F. V.; Suschitzky, H.; Khan, Z. U. *Synthesis* **1977**, 757.
(17) Schrock, A. K.; Schuster, G. B. *J. Am. Chem. Soc.* **1984**, *106*, 5234.
(18) Dunkin, I. R.; Thomson, P. C. P. *J. Chem. Soc., Chem. Commun.* **1980**, 499.
(19) Maltsev, A.; Bally, T.; Tsao, M.-L.; Platz, M. S.; Kuhn, A.; Vosswinkel, M.; Wentrup, C. *J. Am. Chem. Soc.* **2004**, *126*, 237.
(20) Tsao, M.-L.; Platz, M. S. *J. Phys. Chem. A* **2004**, *108*, 1169.

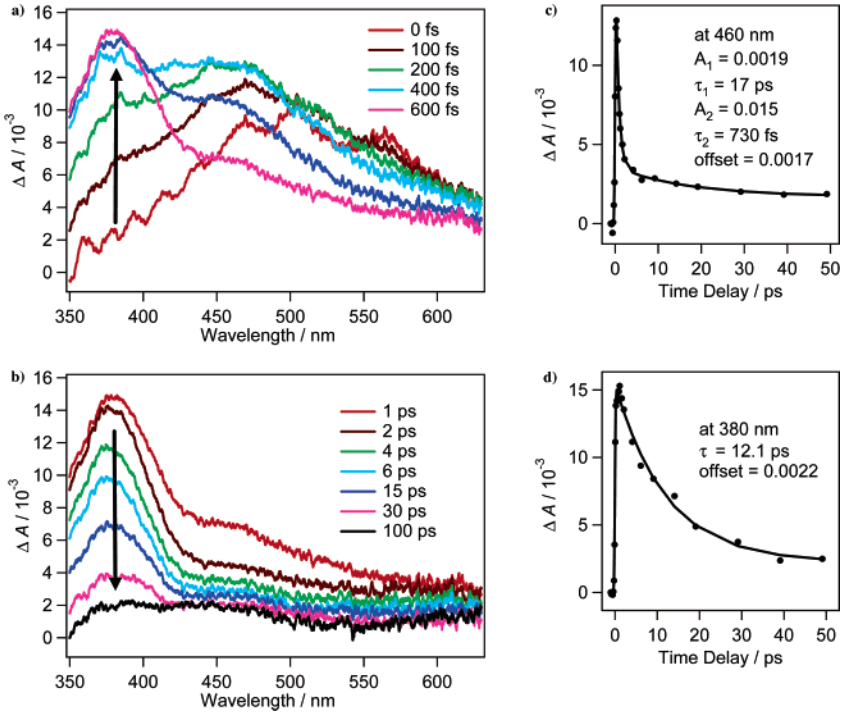

Figure 9. Transient absorption spectra recorded in (a) 0−0.6 ps and (b) 1−100 ps time windows for 1-naphthyl azide in acetonitrile. Graphs (c) and (d) represent kinetic traces at 460 and 380 nm.

Nanosecond (ns) time-resolved laser flash photolysis of 1-naphthyl azide (**1NA**) in 3-methylpentane at 77 K produces singlet 1-naphthylnitrene (**^{1}1NN**) (λ_{max} = 362, 383, and 397 nm) within the 5−10 ns time resolution of the experiment.[20] CASSCF calculations[20] predict that **^{1}1NN** absorbs strongly at 342, 411, and 493 nm in fair agreement with experiment. At 77 K, **^{1}1NN** relaxes to the lower energy triplet state (**^{3}1NN**). The gas-phase, singlet−triplet energy separation, ΔE_{ST}, is predicted to be 13.9 kcal/mol by CASPT2//CASSCF(12,12)/6-31G* calculations,[19] and for which the triplet is the ground state. This energy separation is smaller than the calculated and experimentally determined singlet−triplet splitting of phenylnitrene[21−24] (17−18 kcal/mol).

The intersystem crossing (ISC) rate constant of **^{1}1NN** is $(1.1 \pm 0.1) \times 10^7$ s^{-1} at 77 K and is not expected to be sensitive to temperature.[20] The triplet nitrene has been well characterized by matrix EPR,[25] IR, and UV−vis spectroscopic methods,[19,20] and, in the latter two cases, the spectra have been adequately simulated by modern theory.[19,20]

At ambient temperature, singlet 1-naphthylnitrene cyclizes faster to form naphthazirine **1NAZ** (Scheme 5) than it will relax to **^{3}1NN**.[19,20] The calculated barrier to cyclization is 5.5 kcal/mol, as predicted by CASPT2//CASSCF(12,12)/6-31G* calculations.[19,20] LFP of **1NA** at ambient temperature forms the azirine **1NAZ**, which was detected by time-resolved IR spectroscopy

Scheme 5

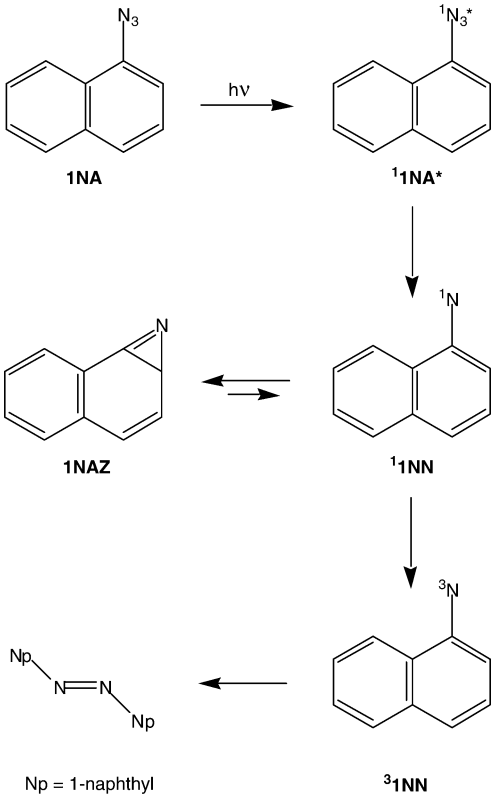

(1728 cm^{-1}).[20] Triplet nitrene **^{3}1NN** is formed 2.8 μs after the laser pulse,[17,20] presumably by equilibration of **1NAZ** and **^{1}1NN** followed by intersystem crossing (ISC) (Scheme 5). Naphthazirine **1NAZ** has been characterized by both matrix IR and UV−vis spectroscopic methods.[19,20] Unlike the benzazirines, the ring expansion of naphthazirines to cyclic ketenimines is endothermic, and this reaction is not observed in solution at

(21) (a) Travers, M. J.; Cowles, D. C.; Clifford, E. P.; Ellison, G. B. *J. Am. Chem. Soc.* **1992**, *114*, 8699. (b) McDonald, R. N.; Davidson, S. J. *J. Am. Chem. Soc.* **1993**, *115*, 10857.
(22) Kim, S.-J.; Hamilton, T. P.; Schaefer, H. F. *J. Am. Chem. Soc.* **1992**, *114*, 5349.
(23) Hrovat, D. A.; Waali, E. E.; Borden, W. T. *J. Am. Chem. Soc.* **1992**, *114*, 8698.
(24) Castell, O.; García, V. M.; Bo, C.; Caballol, R. *J. Comput. Chem.* **1996**, *17*, 4.
(25) (a) Wasserman, E. *Prog. Phys. Org. Chem.* **1971**, *8*, 319. (b) Coope, J. A. R.; Farmer, J. B.; Gardner, C. L.; McDowell, C. A. *J. Chem. Phys.* **1965**, *42*, 54. (c) Kuzaj, M.; Luerssen, H.; Wentrup, C. *Angew. Chem., Int. Ed. Engl.* **1986**, *25*, 480.

ambient temperature. Photolysis of naphthazirines immobilized in cryogenic matrices does, however, lead to the formation of cyclic ketenimines (benzodidehydroazepines).[19]

Ultrafast LFP of **1NA** ($A = 0.65$ at 266 nm) in acetonitrile produces the transient spectra of Figure 9. The transient absorption band centered at 460 nm is formed within the time resolution of the spectrometer (300 fs). We attribute the transient absorption spectrum observed at 460 nm at early delay times to the S_2 state of **1NA**. This excited-state species decays with a time constant of 730 fs. The spectral position of the excited azide S_2 ($\pi \rightarrow (\pi^*,\text{aryl})$) of **1NA** is not far from the S_1 ($\pi \rightarrow \pi^*$) absorption of naphthalene (see Figure S1 in the Supporting Information).

At longer delay times (>3 ps), only the 385 nm band is observed. The carrier of this species can be assigned with confidence to the absorption of **^{1}1NN**, previously observed by nanosecond time-resolved LFP of **1NA** at 77 K. This spectrum is broader than that observed by nanosecond spectroscopy at 77 K;[20] however, this is not troubling as sharper spectra are invariably obtained at cryogenic temperature relative to ambient temperature. An isosbestic point in the ultrafast data is observed at 410 nm, but it is less obvious than for **PBA** and **OBA**, as the absorption spectra of **^{1}1NA*** in the S_2 state and **^{1}1NN** overlap significantly. The transient absorption of **^{1}1NN** at 385 nm decays with a time constant of 12 ps (Figure 9d) at ambient temperature to form naphthazirine (**1NAZ**). **1NAZ** absorbs strongly below 300 nm and cannot be detected in this study (that is, the absorption is outside our spectral probe range of 350−620 nm). Evidence of vibrational cooling of **^{1}1NN** (e.g., spectral envelope rephasing) is not present. Indeed, normalization of the **^{1}1NN** absorption band, at its maximum amplitude (to eliminate the contribution of the 12 ps component), does not show any band narrowing effect. Thus, either **^{1}1NN** is formed thermally relaxed or it is formed vibrationally excited and isomerizes to naphthazirine (**1NAZ**) at the same rate that it undergoes vibrational relaxation.

Deuteration of the solvent has no discernible influence on the observed dynamics ($\lambda_{ex} = 270$ nm, $\tau_1 = 0.8$ ps, $\tau_2 = 15$ ps).

III. Conclusions

UV photolysis of *ortho*- and *para*-biphenylyl azide and 1-naphthyl azide excites the aromatic azides to their S_2 states, which are $\pi \rightarrow (\pi^*,\text{aryl})$ in nature. These states absorb broadly in the visible and have lifetimes of hundreds of femtoseconds. They decay by internal conversion to the lower energy S_1 states which are $\pi \rightarrow$ (in-plane,π^*,azide) in nature. These states are not detected as they immediately fragment (over a 2 kcal/mol barrier) to form molecular nitrogen and the corresponding singlet arylnitrenes. The rate of decay of the S_2 state of the azides is the same as the rate of formation of the singlet nitrenes. Singlet *para*-biphenylnitrene is formed with excess vibrational energy and undergoes vibrational cooling in 11 ps. Singlet *ortho*-biphenylnitrene and 1-naphthylnitrene have lifetimes of 16 and 15 ps, respectively. These nitrenes disappear at a rate comparable to that of vibrational cooling.

IV. Experimental and Computational Methods

IV.1. Computational Methods. Geometry optimizations were performed with the TURBOMOLE 5.71 suite of programs for electronic structure calculations.[26,27] The geometries of the ground states were optimized using the approximate second-order coupled-cluster wave function model using the resolution-of-the-identity approximation (RI) for the electron repulsion integrals (RI-CC2)[5] and with the hybrid density functional, B3LYP.[6] In the RI-CC2 calculations, a frozen-core approximation was employed in which the 1s electrons of C and N atoms were excluded from the correlation treatment. The TZVP ([11s6p1d]/[5s3p1d] for C, N and [10s]/[4s] for H) basis sets of Ahlrichs and co-workers[26] were used for all calculations.[28,29] The equilibrium geometries for the excited states were optimized using recent implementations of analytical gradients for RI-CC2[30,31] and time-dependent density functional theory (TD-DFT) in TURBOMOLE.[32−35] Ground-state vibrational frequency calculations were computed using the analytical second-derivative program AOFORCE. When possible, the vibrational frequencies of the stationary points on the excited-state potential energy surfaces were computed by numerical differentiation of the analytical gradients for the RI-CC2 and TD-DFT for geometries displaced by central differences (0.02 a.u.). Minima were characterized to have all real vibrational frequencies. CASSCF(4,6) calculations with the SVP basis set were performed with the Gaussian 03 suite of programs.[36]

IV.2. Femtosecond Broadband UV−Vis Transient Absorption Spectrometer. The laser system (see Figure S2 of the Supporting Information) consists of a short pulse titanium-sapphire oscillator (Coherent, Mira) generating 30 fs pulses at 800 nm that seeds a high-energy titanium-sapphire regenerative amplifier (Coherent/Positive Light, Legend HE USP). The regenerative amplifier produces 2.5 mJ, 40 fs pulses at 1 kHz. The main part of the beam is used to pump two OPAs (OPerA Coherent) equipped with UV−vis and SFG modules, respectively, allowing us to generate a pump pulse tunable from 240 to 800 nm. A small portion of the fundamental is used for white light generation in the range 320−700 nm by focusing a small portion of the fundamental output (800 nm, 1.5 μJ) into a 1 mm thick CaF_2 plate. To create a stable white light continuum, the fundamental power density in the focus is carefully adjusted and each 3 s the CaF_2 rotates by a small angle of 1.5°. A 50 mm lens collimates the white light continuum beam, which then passes through an iris to select the central, uniform region of the beam profile. The white light continuum is split into two parts, probe and reference, of nearly equal intensity by using reflection from the front (probe) and back (reference) surfaces of a 6 mm thick CaF_2 plate. Both beams pass through the sample, but only the probe overlaps with the pump beam in the sample.

The sample is circulated in a Harrick Scientific flow cell (1 mm thick CaF_2 windows), and the optical path length was 1 mm. The angle between pump and probe beam is 5°. To avoid rotational diffusion effects, the angle between polarizations of the pump beam and the probe beam was set to the magic angle (54.7°)[37] by rotating a $\lambda/2$ waveplate.

The detection system consists of an imaging polychromator (Triax 550 Jobin Yvon, equipped with holographic grating operating in 250−800 nm, 150 gr/mm) and thermoelectrically cooled, back illuminated CCD camera (Symphony Jobin Yvon, chip 2048 × 512 pixels). Both the probe and the reference are focused on the entrance slit (0.5 mm wide) and detected on a separate vertical region of the CCD chip. Ratioing of the two spectra minimizes noise due to white light

(26) (a) Ahlrichs, R.; Bär, M.; Häser, M.; Horn, H.; Kölmel, C. *Chem. Phys. Lett.* **1989**, *162*, 165. (b) For the current version of TURBOMOLE, see http://www.turbomole.de.
(27) Treutler, O.; Ahlrichs, R. *J. Chem. Phys.* **1995**, *102*, 346.
(28) Schäfer, A.; Huber, C.; Ahlrichs, R. *J. Chem. Phys.* **1994**, *100*, 5829.
(29) Eichkorn, K.; Weigend, F.; Treutler, O.; Ahlrichs, R. *Theor. Chem. Acc.* **1997**, *97*, 119.
(30) Hättig, C.; Weigend, F. *J. Chem. Phys.* **2000**, *113*, 5154.
(31) Hättig, C.; Köhn, A. *J. Chem. Phys.* **2002**, *117*, 6939.
(32) Furche, F.; Ahlrichs, R. *J. Chem. Phys.* **2002**, *117*, 7433.
(33) Furche, F.; Ahlrichs, R. *J. Chem. Phys.* **2004**, *121*, 12772.
(34) Hättig, C. *J. Chem. Phys.* **2003**, *118*, 7751.
(35) Köhn, A.; Hättig, C. *J. Chem. Phys.* **2003**, *119*, 5021.
(36) Frisch, M. J.; et al. *Gaussian 03*, revision C.02; Gaussian, Inc.; Wallingford, CT, 2004.
(37) Lessing, H. F.; von Jena, A. *Chem. Phys. Lett.* **1976**, *42*, 213.

continuum fluctuations. A shutter (Uniblitz) set in the pump beam minimizes the sample irradiation time, while a shutter set in the probe beam permits background and emission measurements (white light continuum OFF, pump ON). To increase the signal-to-noise ratio of recorded transient absorption spectra, a modulation technique is used. The CCD camera acquisition is referenced to an optical chopper (New Focus 3501) placed in the probe beam (25 Hz), which operates in synchronization with another chopper placed in the pump beam (12.5 Hz). Probe and reference spectra are integrated during a 20 ms exposure, and an additional 20 ms is required to reset the CCD for the next acquisition. At a given pump−probe delay, 250 acquisitions are taken with every other acquisition recorded with the presence of the pump. Spectra with and without the pump are used to calculate a transient absorption spectrum. This modulation method results in a very good signal-to-noise ratio, so amplitudes smaller than 0.001 absorbance could be measured.

Transient absorption spectra are recorded at different pump−probe delay times using an optical delay line consisting of computer-controlled, motorized translation stage mounted with a retroreflector. The entire set of pump−probe delay positions (cycle) is repeated at least three times, to observe data reproducibility from cycle to cycle.

Spectra are recorded using home-developed software, written in Labview 7.0, which also controls the optical delay line, shutters, CaF_2 rotation, and CCD acquisition.

The absorbance of the sample solutions is typically 0.6−0.7 at the excitation wavelength, and the sample volume is 50 mL. Pump pulse energy is about 6 μJ at the sample position. Transient absorption spectra are corrected for chirp in the probe continuum.[38] Kinetic traces are analyzed by fitting to a sum of exponential terms, $S(t) = \sum A_i \exp(-t/\tau_i) + C$, with independent amplitudes, A_i, lifetimes, τ_i, and offset, C. Convolution with a Gaussian response function is included in the fitting procedure. The instrument response fwhm is approximately 300 fs. All experiments are performed at room temperature.

IV.3. Materials. All of the azides[39] are known and were synthesized and purified by the methods described elsewhere.[1,2,5,10,15−17] Acetonitrile (Sigma-Aldrich, spectrophotometric grade) was used as received. Acetonitrile-d_3 was purchased from Cambridge Isotopes.

Acknowledgment. This work was performed at The Ohio State University Center for Chemical and Biophysical Dynamics (CCBD) and The Ohio Supercomputer Center. Support of this work, and of the CCBD, by the National Science Foundation is gratefully acknowledged. We gratefully acknowledge fruitful discussions with Andreas Köhn (Kemisk Institut, Aarhus Universitet).

Supporting Information Available: Ultrafast LFP transient spectra of naphthalene, additional computational data, Cartesian coordinates of the geometries discussed herein, and complete ref 36. This material is available free of charge via the Internet at http://pubs.acs.org.

JA061520I

(38) Nakayama, T.; Amijima, Y.; Ibuki, K.; Hamanoue, K. *Rev. Sci. Instrum.* **1997**, *68*, 4364.

(39) Talrose, V.; Yermakov, A. N.; Usov, A. A.; Goncharova, A. A.; Leskin, A. N.; Messineva, N. A.; Trusova, N. V.; Efimkina, M. V. UV/Visible Spectra. In *NIST Chemistry WebBook, NIST Standard Reference Database Number 69*; Linstrom, P. J., Mallard, W. G., Eds.; National Institute of Standards and Technology: Gaithersburg, MD, 2005.